Application of a Novel Linear/Exponential Hybrid Force Field Scaling Scheme to the Longitudinal Raman Active Mode of Polyyne

Shujiang Yang and Miklos Kertesz*

Department of Chemistry, Georgetown University, Washington, DC 20057-1227

Viktor Zólyomi† and Jenő Kürti

Department of Biological Physics, Eötvös University Budapest, Pázmány Péter sétány 1/A, H-1117 Budapest, Hungary

Received: November 27, 2006; In Final Form: January 9, 2007

The properties of an infinite carbon chain (polyyne), an allotropic form of elemental carbon, are of importance in materials science as well as astronomy. The Raman active longitudinal optical (LO) frequencies are calculated with first-principles methods for oligoynes and polyyne and compared with experiments. Since traditional force constant scaling schemes fail in this case, we introduced a linear/exponential scaling scheme based on the exponential behavior of the carbon−carbon bond stretching force constant couplings in quasi-one-dimensional conjugated chains. The LO Raman active frequency is predicted at 1870−1877 cm^{-1}. Our results provides further evidence for the assignment of the characteristic Raman peaks near 1850 cm^{-1} of the recently discovered long linear carbon chains encapsulated inside multiwalled or double-walled carbon nanotubes.

1. Introduction

Little is known about the properties of very long carbon chains that form the sp-hybridized allotrope of the element of life. From the perspective of formal chemical valency of carbon, two forms of infinite carbon chains might exist based on the pair of π orbitals on each C atom oriented perpendicular to the chain axis: *polycumulene*, $(=C=)_x$, an equidistant carbon chain, and *polyyne*, $(-C\equiv C-)_x$, which features a triple−single bond alternating pattern. Because of its symmetry, polycumulene has a half-filled metallic band structure, while polyyne is expected to have a sizable band gap, making it a semiconductor. All calculations[1−5] indicate that polyyne is more stable than polycumulene because the latter has a degenerate pair of half-filled energy bands that are subject to Peierls distortion.[6] Experimentally, the study of polyyne has been hampered by the high reactivity of multiple bonds, although many publications have claimed the synthesis of polyyne, with observed carbon−carbon stretching Raman bands at 2000−2200 cm^{-1} serving as evidence.[7−9]

Very long carbon chains have been directly observed inside multiwalled carbon nanotubes by high-resolution transmission electron microscopy (HRTEM) recently.[10,11] Zhao et al.[10] found two Raman peaks associated with the encapsulated carbon chains one at 1825 cm^{-1} and another around 1855 cm^{-1} (the latter can be decomposed into two peaks at around 1850 and 1860 cm^{-1} after a Lorentzian fit). These bands are polarized along the chain direction and are resonantly enhanced at around 2.5 eV.[10] Jinno et al.[12] observed the same Raman peaks at 1829 and 1857 cm^{-1} for multiwalled carbon nanotubes and at 1829 and 1855 cm^{-1} for double-walled carbon nanotubes. They also found that these bands are resonantly enhanced at 2.4 eV and are related to chainlike materials inside multiwalled and double-walled carbon nanotubes. The resonant Raman excitation energy should be close to the band gap of polyyne, which we estimate to be around 2.2 eV based on the extrapolation from optical absorption experiments reported for short oligomer carbon chains (oligoynes)[13−15] and theoretical predictions.[16] Zhao et al.[10] assigned these two Raman peaks to the longitudinal optical (LO) mode of long linear carbon chains consisting of more than 40 atoms with alternating and nonalternating structures.[10] However, this assignment is not consistent with former experimental results[7−9] and limited theoretical vibrational predictions[2,3,5] for polyyne. In addition, a monatomic linear chain, such as polycumulene, has only acoustic phonon branches, so it cannot have any spectroscopically allowed vibrational modes[17−20] despite the fact that various Raman peaks below 2000 cm^{-1} have been assigned to polycumulene before.[21] Liu et al.[22a] suggested assigning the two Raman peaks[10,12] around 1850 cm^{-1} to short oligoynes based on density functional theory (DFT) calculations. Such an interpretation cannot explain the HRTEM observation[10] indicating the presence of long chains. Fantini et al.[22b] also observed intense Raman peaks around 1850 cm^{-1} resonantly enhanced around 2.2 eV at similar materials synthesis conditions, which they assigned to short carbon chains interconnecting carbon nanotube surfaces. To clarify this issue, it is essential to obtain reliable vibrational predictions for the LO mode frequency of polyyne with state-of-the-art quantum mechanical calculations.

In this paper, we investigate the Raman active LO stretching vibrational modes of linear carbon chains with the aid of quantum mechanical calculations. The LO frequency of oligomers changes hundreds of wavenumbers as a function of size. This necessitates the use of unusually long oligomers in this work in order to achieve convergency as a function of size. By comparing the results with experiments for intermediate-sized

* Corresponding author. E-mail: kertesz@georgetown.edu. Telephone: 202-687-5761. Fax: 202-687-6209.

† Present address: Research Institute for Solid State Physics and Optics of the Hungarian Academy of Sciences, P.O.B. 49, H-1525, Budapest, Hungary.

10.1021/jp067866x CCC: $37.00
Published on Web 02/24/2007

oligoynes, we develop a novel scaling scheme that provides an excellent fit for known frequencies and yields extrapolations for the infinite chain that are comparable to the experimental frequencies found for the carbon chains inside nanotubes mentioned above. As a byproduct, we obtained some insights into limitations of some of the widely used methods for vibrational calculations.

2. Theoretical Methods

There are unusual difficulties in theoretically calculating the vibrational frequencies of polyyne. The physically most apparent difficulty is the requirement for accurately describing the *bond length alternation* (BLA $= R_s - R_t$, the difference between the length of single and triple bonds) and the associated energy band gap. This problem depends strongly on electron correlation and electron phonon coupling for 1-D conjugated systems not only for polyyne but also for polyacetylene (PA) and other conjugated polymers.[23] The selection of the method is critical in this regard, for instance, Hartree−Fock (HF) overestimates the BLA, and various DFT methods including the local density approximation (LDA) and generalized gradient approximation (GGA) significantly underestimate it.[24] In addition, for longer oligomers, we had to overcome the notorious *basis set linear dependency* problem[25−29] for carbon chains[2,4] due to large overlaps generated by the short bond lengths. The third problem is the *slow convergence* of vibrational modes with respect to the *size* of oligoynes. We have employed molecular packages for the oligomer calculations. Two approaches were used.

The first is the *direct oligomer approach* where a normal-mode frequency of a polymer is obtained by extrapolating the corresponding mode's frequencies from a series of finite oligomers to the infinite size limit. Calculations on a series of oligoynes with finite chain length are performed by the Gaussian03 program[30] with Gaussian-type basis sets. Extrapolations are then performed by fitting the relevant LO mode frequencies as a function of inverse chain length. The selection of the theoretical levels is limited due to the need for including very long oligomers. We used various forms of nonhybrid *and* hybrid DFT (B3LYP of the B3 hybrid scheme,[31] BH&HLYP[30] of the half-and-half hybrid scheme) and Hartree−Fock (HF) theory.

The direct oligomer approach is straightforward, but it converges slowly (see Results Section). Therefore, we developed a second approach over the years which we have called the *Polycalc approach*, which reduces the size of oligomers needed to achieve convergency.[20,32] The *Polycalc* program uses a two-step approach: First, a molecular vibrational calculation is performed on a large oligomer that consists of several repeat units and is terminated by properly chosen end groups. Then, force constant blocks are extracted from the Hessian matrix corresponding to the central part of this oligomer and are used to construct the force field of the corresponding polymer, as illustrated in Figure 1a. The k-dependent dynamical matrix $\tilde{F}(k)$ of the polymer takes the following form assuming periodicity and utilizing periodic boundary conditions (PBC):[18−20]

$$\tilde{F}(k) = F(0,0) + \sum_{q=\pm 1}^{\pm N} F(0,q)\exp(ikqa) \qquad (1)$$

where k is the reciprocal wave vector, a is the translational vector, and $F(p,q)$ is the block of the force constant matrix referring to the couplings between the pth and qth repeat unit. $F(p,p)$ contains the diagonal and off-diagonal force constants within the pth unit. The summation usually extends over all N neighbors for which force constants are available except for the blocks closest to the terminal groups to minimize end effects. This summation usually converges very fast and only a few neighbors are needed. However, as we shall show in the case of polyyne, we need to include contributions from a number of extended neighbors. All matrices in eq 1 are $3M \times 3M$, where M is the number of atoms in the repeat unit. Periodicity would mean that $F(p,q) - F(0,q-p) = 0$. In reality, this difference for finite oligomers is small but not zero, although with increasing oligomer size, the difference goes to zero for properly capped oligomers. The elements of $F(p,q)$ are described in Cartesian coordinates:

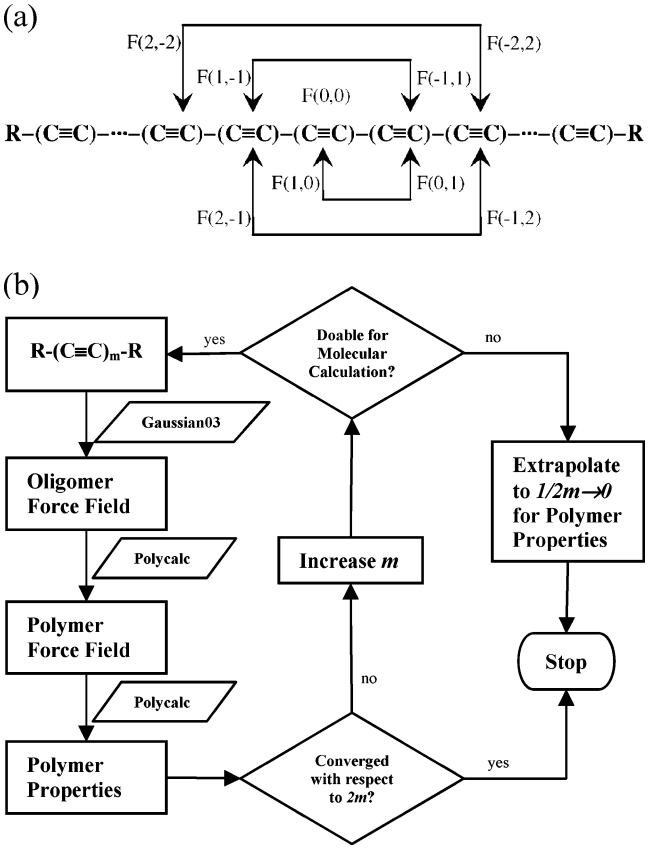

Figure 1. (a) Force constant blocks of polyyne extracted from the Hessian of a sufficiently long and appropriately terminated oligomer. The numbering refers to repeat units starting from the most central unit. The force constant blocks $F(p, q) = F(0, q-p)$ as used in eq 1. (b) Schematic diagram of the process used in the Polycalc approach.

$$F_{i,j}(p,q) = \frac{\partial^2 E}{\partial X_{i,\mathrm{p}} \partial X_{j,q}} \qquad (2)$$

To minimize end group effects and maximize the number of neighboring unit cell force constant couplings, the reference unit cell ($p = 0$) is chosen to be in the middle and the coupling blocks are chosen to be as symmetrical around it as possible. As shown in Figure 1a, force constant coupling $F(-1,1)$ is selected to represent $F(0,2)$; $F(-1,2)$ is selected to represent $F(0,3)$ in eq 1, etc.

Solid-state k-dependent vibrational calculations of the polymer are performed based on these extracted $F(p,q)$ blocks in eq 1, following the k-dependent version of Wilson's GF matrix method:[33]

$$\tilde{F}(k)C_i(k) = \omega_i^2(k)GC_i(k) \qquad (3)$$

where G is a diagonal mass matrix of the unit cell, $C_i(k)$ is the ith eigenvector for the respective normal mode, $\omega_i(k)$ is the eigenvalue for the ith phonon branch at k with the value $\omega_i(k) = 2\pi\ \nu_i(k)$, and $\nu_i(k)$ is the frequency of the ith phonon branch at k.

According to the selection rules for polymers,[18] only the $k = 0$ (Γ point) frequencies are IR or Raman-allowed transitions. For most polymeric systems, the $k = 0$ state frequencies obtained through Polycalc converge much faster than with the direct oligomer approach, which is behind the success of this approach.[32,34,35] However, for the highly conjugated carbon chain system, as we will demonstrate in the next section, convergency can still be slow. Additional extrapolations of the $k = 0$ mode frequency with respect to the chain length are performed to check the convergency of results from the longest oligomers. The complete process of the Polycalc approach is illustrated in Figure 1b.

Corresponding to the $k = 0$ LO mode frequency of polyyne, there is one LO mode for each oligoyne, which is an in-phase C≡C stretching mode where adjacent single/triple bonds are being stretched/compressed with opposite phases. Such a mode has a large Raman intensity and is the closest to the $k = 0$ LO phonon mode of the respective infinite chain. This important mode will be referred to as the *in-phase LO mode* in this paper.

Only after we obtained the converged harmonic frequencies could we turn to the question of comparison with experiment and the choice of a *proper scaling method* in order to achieve good agreement with experimental frequencies. Standard and new scaling algorithms will be discussed in Part 3.

3. Results and Discussion

3.1. Hybrid DFT Predictions for the LO mode Frequency of Polyyne. The B3-type hybrid DFT functionals[31] have been proven to be the most reliable theory for vibrational predictions among several alternatives studied, including MP2, QCISD, and various DFT at GGA or LDA levels.[36,37] However, despite some early work in this field[29,38,39] there is no publicly tested program for solid-state *vibrational* calculations at B3LYP level. Therefore, we chose the direct oligomer approach and the Polycalc approach with the B3LYP/6-31G* theory. The respective frequencies are presented as a function of $x = 1/2m$ in Figure 2 based on a series of H-(C≡C)$_m$-H oligoynes with up to $2m = 72$.

In the direct oligomer approach, the $k = 0$ LO mode frequency of polyyne is extrapolated from the $x = 1/2m$ dependency of the in-phase LO mode frequencies of oligoynes to the $x \rightarrow 0$ limit. A quadratic fit in x gave 1795 cm^{-1} based on the frequencies in the $34 \leq 2m \leq 72$ region. The alternative Polycalc approach converges visibly faster and yields a satisfactorily close value of 1797 cm^{-1} in the $1/2m \rightarrow 0$ limit based on the oligomers sized $48 \leq 2m \leq 72$.

Even though the direct oligomer approach and Polycalc use the same oligomer Hessian at any given size, the Polycalc frequencies converge faster because of the PBC used in the vibrational part of the calculation. To our knowledge, H-(C≡C)$_{36}$-H is the longest oligoyne ever studied in the literature for first-principles frequency calculations that appears to be adequately long to perform the extrapolation to infinite size with sufficient accuracy. The slow pace of the convergency is apparent in both cases from Figure 2. It explains why there are different values reported in the literature when different-sized oligomers are adopted. For instance, using oligomers up to $2m = 40$, the extrapolation to infinite size could differ from the value obtained from up to $2m = 72$ oligomers by ~100 cm^{-1}.

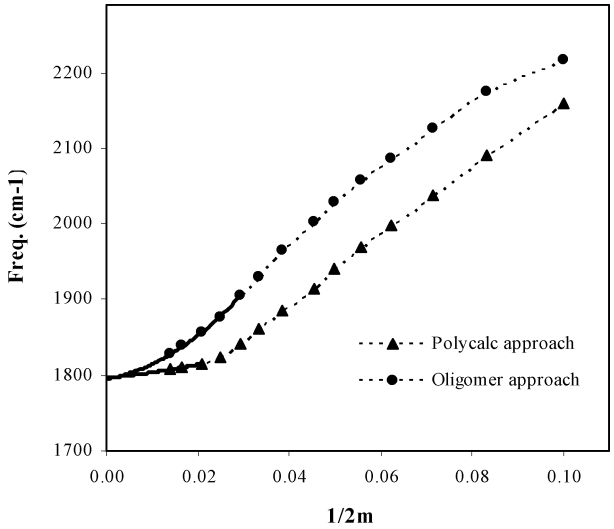

Figure 2. Extrapolation process to obtain the $k = 0$ LO mode frequency of polyyne at the *unscaled* B3LYP/6-31G* level through the direct oligomer approach (circles) and the Polycalc approach (triangles) as a function of the inverse size $1/2m$ of H-(C≡C)$_m$-H ($2m$ up to 72) oligoynes. Dashed lines are drawn to guide the eye. Solid lines are quadratic fits in terms of $1/2m$ on large oligoynes with R^2 factors over 0.9994. Note the faster convergency of the Polycalc approach at $1/2m \rightarrow 0$ limit.

Generally, coupling force constants are localized, and they are only weakly affected by farther lying chemical groups, as evidenced by the usually fast convergency of eq 1. The highly conjugated polyyne system is found to be very different. As we shall see in this paper, couplings with q values of up to 9−12 still have a significant effect on the LO mode frequency. There are clearly some longer-range coupling effects at work in this case, which have also been found in other conjugated systems such as porphine[40] and polyacetylene.[41]

There are two factors affecting the convergence of the $k = 0$ LO mode frequencies to the $1/2m \rightarrow 0$ limit: convergency as a function of the number of included neighboring repeat unit couplings, and convergency of the force constants themselves as the size of the oligomer increases. Merely for the purpose of analysis, we separated these two effects using the Polycalc approach at the B3LYP/6-31G* level in Figure 3. Figure 3a shows the dependence of the $k = 0$ LO mode frequency of polyyne as a function of the number of $F(0,q)$ blocks, N, included in the force field. All the Hessians for different N values are taken from the central part Hessian of the extremely long oligoyne H-(C≡C)$_{36}$-H. Convergency is achieved only when at least $N = 9-10$ unit cell force constant couplings (or 19−21 carbon−carbon atomic neighbors) are included. In Figure 3b, the number of unit cell couplings is constrained to $N = 4$ and the size of the oligomer is varied in order to show the effect of the changes in the force constants themselves as a function of size in the $2m = 10-72$ region. Convergency of up to spectroscopically useful accuracy (a few cm^{-1}) is only achieved with large oligomers, $2m \geq 60$. While both factors in Figure 3a and b converge slowly, it is clear that the slow convergency of the $k = 0$ LO mode frequency is mainly caused by the slow convergency of the force constants as shown in Figure 3b because the $N = 9$ condition can be fulfilled by oligomers in the Polycalc approach with oligomers as short as $2m = 24$.

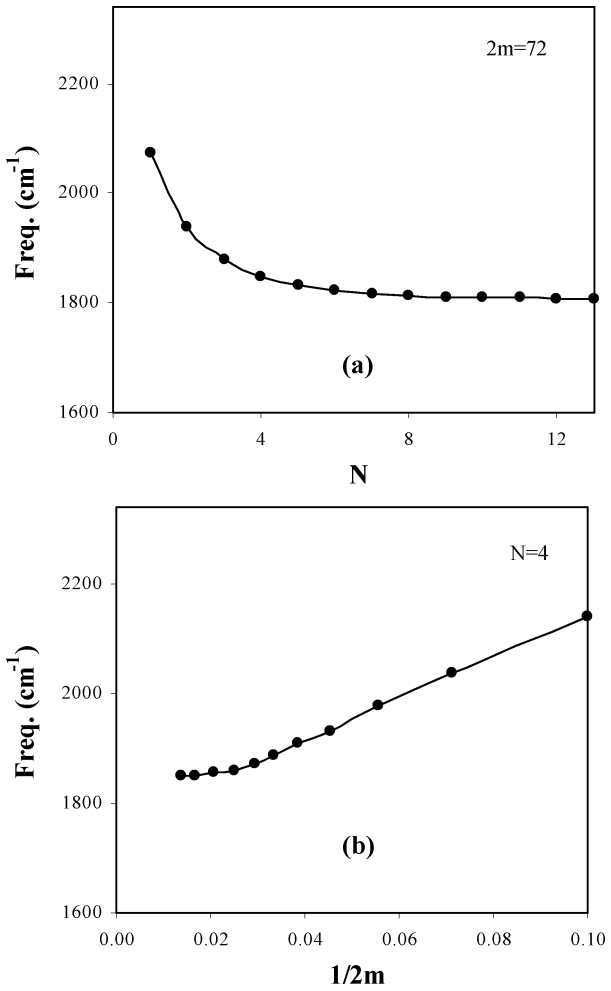

Figure 3. Convergency of the $k = 0$ LO mode frequency of polyyne revealed in the Polycalc approach at B3LYP/6-31G* level: (a) as a function of number of neighboring unit cell couplings, N, as defined in eq 1 using the Hessian of the H-(C≡C)$_{36}$-H oligomer; (b) as a function of the inverse size $1/2m$, with fixed number of neighboring couplings ($N = 4$).

3.2. SQM Scaling Results for the LO Mode Frequency. Theoretical vibrational results should be scaled to be comparable with experiments due to limitations of theory, basis set truncation, anharmonicity, etc. There are currently two popular scaling schemes. The first is the uniform frequency scaling, which is straightforward and convenient:

$$\nu^{\text{scaled}} = \nu^{\text{unscaled}} s \tag{4}$$

where the frequency scaling factor s for B3LYP/6-31G* is determined to be around 0.96.[36,37,42]

Pulay's scaled quantum mechanical (SQM) scaling scheme[43,44] is the other popular scaling method and is more accurate. In this method, the original force constant matrix calculated in Cartesian coordinates is transformed into the representation with a set of internal coordinates. Multiple parameter scaling is applied to the elements of the force constant matrix in terms of chemically meaningful internal coordinates:

$$F_{Q_i,Q_j}^{\text{scaled}} = F_{Q_i,Q_j}^{\text{unscaled}} \sqrt{s_i s_j} \tag{5}$$

where s_i and s_j are scaling factors for internal coordinates Q_i and Q_j, respectively. Initially, the set of Q_i was made nonredundant by including individual bond stretches and suitable linear combinations of bends and torsions. When the SQM scheme became capable of performing force constant scaling in the full set of redundant internal coordinates, which includes the entire set of bond stretches, bends and torsions,[44] it became more effective and reliable by removing the necessity and arbitrariness in defining the set of nonredundant natural or group internal coordinates. Optimal scaling factors s_i for various primitive stretching, bending and torsional force constants were derived by a least-square fit of a training set of 663 frequencies for 30 molecules and the s_i values were found to be transferable.[44] After scaling, the scaled force constant matrix in internal coordinates is transformed back to the Cartesian coordinate representation, and a normal GF matrix method is used to solve the scaled normal-mode frequencies.

The harmonic LO mode frequency obtained in this work was initially scaled with the SQM scheme[44] in a full set of redundant internal coordinates. The bending and torsional internal coordinates of the linear chain, being either 0° or 180°, are not included in the redundant set of coordinates because they will pose problems for the nonsymmetrical matrix transformation process. These internal coordinates do not affect the scaling of LO mode frequencies. Oligoynes, except diminutive contributions from end groups, have only two kinds of longitudinal internal coordinates, C≡C (R_t) and C−C (R_s) bond stretches, which are involved in the LO mode. Since diagonal scaling factors for single (s) and triple (t) carbon−carbon bonds are the same in SQM ($s = t = 0.9207$),[44] for medium to long oligoynes and polyyne, the SQM scaling scheme essentially reduces to uniform scaling. The scaling result from SQM is also consistent with uniform scaling (frequency scaling factor $(0.9207)^{1/2}$ vs 0.96) for those cases. The LO mode frequency of polyyne is determined to be 1722 cm^{-1} with the direct oligomer approach and 1724 cm^{-1} with the Polycalc approach at the B3LYP/6-31G* level after SQM scaling.

The reliability of this frequency prediction on polyyne is examined next. Vibrational spectra for H-(C≡C)$_m$-H oligoynes are only available for up to $2m = 6$,[45−48] which are too short. Vibrational spectra for longer oligoynes are available with bulky end groups.[49−51] To minimize the effect of the end groups, we chose the Ar-(C≡C)$_m$-Ar ($2m = 4$, 8, 12, 16, 20; Ar = 3,5-disubstituted (RO−) phenyl) oligoynes[51] for comparison between theory and experiments. We selected 11 reliable experimental IR or Raman frequencies related to longitudinal stretching modes with medium or strong intensities. Five of them are in-phase LO modes, one for each oligoyne. Statistics shows the SQM scaling scheme behaves well for the other six not-in-phase-LO modes, with an rms deviation value of 7.7 cm^{-1}. The major discrepancies between theory and experiments come from the in-phase LO modes, which are shown in Figure 4. Although the SQM results and experiments agree reasonably well for the shorter oligoynes in Figure 4, the discrepancy increases significantly with increasing size. The overall rms deviation for the in-phase LO modes of the five oligoynes is 33.4 cm^{-1}. An even larger deviation is expected for the in-phase LO mode at the $1/2m \rightarrow 0$ limit by this SQM scaling scheme. The scissor shape between the SQM scaled calculations and the experiments in Figure 4 is indicative of chain-length-dependent or size-dependent effects, which cannot be properly addressed by the SQM scheme. This effect is also present in unscaled and uniformly scaled quantum mechanical vibrational results of the LO mode frequencies.

We did a series of extensive tests to improve the scaling results for longer oligoynes within the SQM scheme. These efforts included adjusting the scaling factor for carbon−carbon (CC) stretches, and/or utilizing separate scaling factors for C≡C

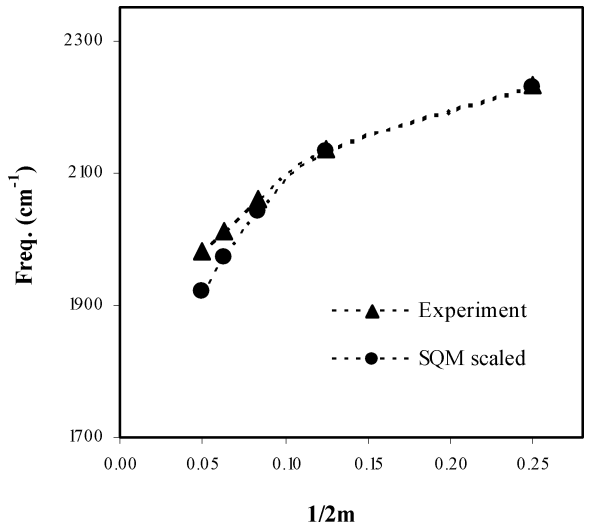

Figure 4. In-phase LO mode frequencies of the Ar-(C≡C)$_m$-Ar (Ar = 3,5-disubstituted (RO-) phenyl) oligoynes scaled by the SQM scheme. Experimental results are taken from ref 51. Lines are drawn to guide the eye.

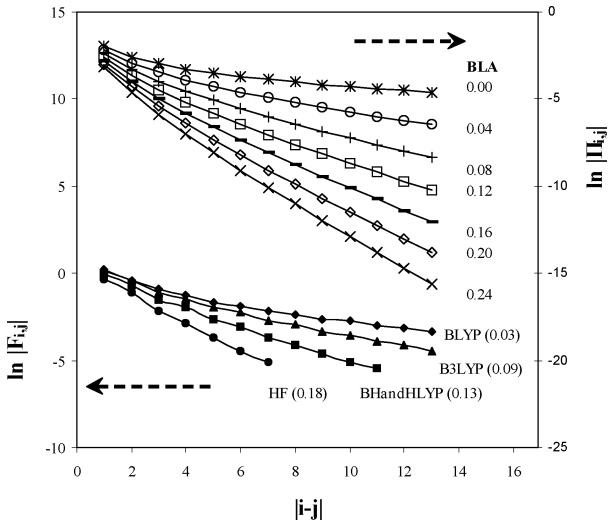

Figure 5. Upper section: logarithm of the mutual bond−bond polarizability, $\ln|\Pi_{i,j}|$, of polyyne as a function of number of neighbors separation ($|i - j|$) and bond length alternation (BLA, in Å) using modified Hückel theory. Lower section: logarithm of the coupling bond-stretching force constants, $\ln|F_{i,j}|$ as a function of $|i - j|$ from first-principles calculations. The values in the parentheses refer to optimized BLA values in Å. Force constant matrix $F_{i,j}$ is extracted from vibrational calculations on H-(C≡C)$_{30}$-H with 6-31G* basis sets.

and C−C, and/or separate scaling factors for their various couplings (C≡C/C−C, C≡C/C≡C, and C−C/C−C). However, this size-dependent problem could not be completely resolved. A different scaling scheme is needed to describe the LO mode appropriately.

3.3. Hybrid Linear/Exponential Scaling of the LO Mode Frequency. The LO mode frequency is affected by both the diagonal and the off-diagonal force constant matrix elements. By using separate scaling factors for the two different types of CC stretches, *s* for C−C and *t* for C≡C, the inadequacy of B3LYP/6-31G* theory in describing the diagonal (stretching) force constants can be adequately compensated. However, we need a new scheme to properly describe the off-diagonal coupling force constants which account for the size-dependent problem found with unscaled, uniformly scaled, or SQM scaled calculations for the LO mode frequency.

At the simple tight binding (Hückel) level, the π-component of the off-diagonal internal force constants of polyyne can be treated semianalytically.[52,53] There is a diminutive contribution from the well-localized σ-bonds within first or second neighbors, but the aim of looking at Hückel theory is to gain insight into the force field behavior extending to a longer range that results from the π-contribution. At the Hückel level, the coupling force constant $F_{i,j}$ between bond *i* and *j* is approximately proportional to the mutual bond−bond polarizability $\Pi_{i,j}$.[53] We calculated $\Pi_{i,j}$ as a function of the number of neighboring separation between *i* and *j* ($|i - j|$) using the distance-dependent Hückel theory of Longuet−Higgins and Salem (LHS).[54] This, together with the effect of bond length alternation (BLA) is shown in the upper part of Figure 5. Despite the fact that $\Pi_{i,j}$ oscillates in sign (±) with respect to the parity of $|i - j|$, its absolute value $|\Pi_{i,j}|$ decays approximately exponentially as a function of $|i - j|$ at medium to large BLA. The larger the BLA, the more linear is the curve of $\ln|\Pi_{i,j}|$ vs $|i - j|$, i.e., the decay of $|\Pi_{i,j}|$ as a function of $|i - j|$ is becoming exponential for medium to large BLA values, with faster decays for more alternating chains. For the equidistant carbon chain (BLA = 0), the decay of $|\Pi_{i,j}|$ reduces to an approximately $1/|i - j|$ relationship, which is an artifact due to the metallic property of this system.

The exponential decay of couplings in linear conjugated long carbon chains is also confirmed by first-principles calculations, as shown in the lower part of Figure 5. With the exception of the first neighbor couplings, which contains both π and non-negligible σ electron contributions, $F_{i,j}$ contains a dominant delocalized π-electron contribution that extends over a number of neighbors. The absolute value of the coupling force constant $|F_{i,j}|$ decays approximately exponentially as a function of bond separation $|i - j|$ at various first-principles theoretical levels including HF, BH&HLYP, B3LYP, and BLYP. Noticing the fact that the optimized BLA of polyyne decreases in the order of HF > BH&HLYP > B3LYP > BLYP, and $|F_{i,j}|$ also decays faster with increasing BLA. We do not know a priori which exponent is closer to the exact value, but it is clear that the exponent should have a profound effect on the calculated LO mode frequencies. This provides the motivation for treating the exponent as an adjustable parameter to be determined from a fitting process based on experimental frequencies of long oligomers.

On the basis of the intrinsic behavior of coupling force constants for longitudinal stretching modes, we introduce a novel hybrid linear/exponential (Lin/Exp) scaling scheme to empirically correct the decay of the coupling force constants. Linear scaling is applied to all diagonal internal force constants and off-diagonal internal force constants involving terminal groups as the SQM scheme in eq 5. Separate scaling factors are used for C−C (*s*) and C≡C (*t*). Exponential scaling is applied to the longitudinal off-diagonal coupling force constants between different backbone CC stretches. The hybrid Lin/Exp scaling scheme is described below:

$$F_{i,j}^{\text{scaled}} = F_{i,j}^{\text{unscaled}} \times c^{|i-j|}, \quad \text{when } i \text{ and } j \text{ are different backbone CC stretches} \tag{6a}$$

$$F_{i,j}^{\text{scaled}} = F_{i,j}^{\text{unscaled}} \sqrt{s_i s_j}, \quad \text{for all other cases} \tag{6b}$$

The hybrid Lin/Exp scaling parameters *s* for C−C, *t* for C≡C stretches, and *c* for exponential scaling, are optimized based on the above selected 11 IR or Raman modes of the Ar-(C≡C)$_m$-Ar ($2m = 4-20$) oligoynes.[51] Transverse modes are not discussed in this work. Other scaling factors involving end

TABLE 1: Statistics of the Hybrid Linear/Exponential Scaling on the Carbon Chain System Compared with SQM and Modified SQM Scaling[a]

scaling scheme	SQM	modified SQM	linear/exponential
s (C−C)	0.921	0.934	0.800
t (C≡C)	0.921	0.890	0.950
c (coupling)[b]	0.921	0.805	0.864
rms (in-phase LO) (cm^{-1})	33.4	10.1	5.1
rms (other-LO) (cm^{-1})	7.7	7.2	6.9
rms (all) (cm^{-1})	23.2	8.7	7.6

[a] rms (in-phase LO), rms (other LO), and rms (all) refer to the root-mean-square deviations for the five in-phase LO modes, the six other LO stretching modes, and for all 11 LO Modes of Ar-$(C\equiv C)_m$-Ar ($2m$ = 4, 8, 12, 16, 20), respectively. IR or Raman peaks with medium or strong relative intensity in the experiments were selected (ref 51). [b] For the SQM and modified SQM scheme, c replaces $\sqrt{s_i s_j}$ in eq 5 when $i \neq j$; for the linear/exponential scheme, c is the exponential scaling factor in eq 6a.

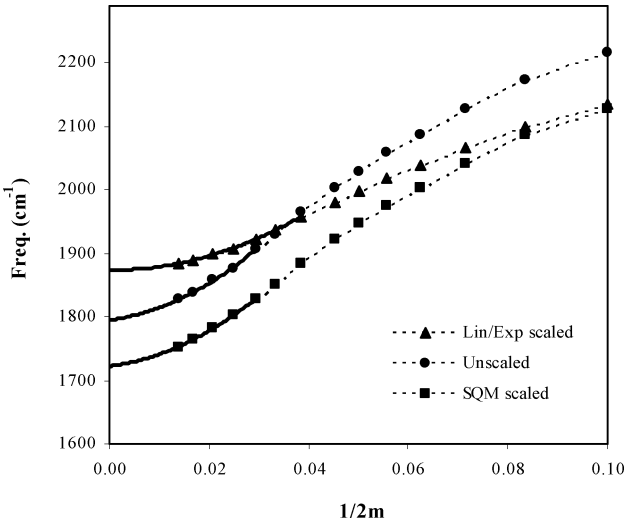

Figure 6. In-phase LO mode frequencies of H-$(C\equiv C)_m$-H oligoynes at the B3LYP/6-31G* level from oligomer calculations as a function of $x = 1/2m$. Frequencies from the linear/exponential hybrid scaling scheme are compared with unscaled and the SQM scaled results. Dashed lines are drawn to guide the eye. Solid lines are quadratic fits in terms of x on large oligoynes with R^2 values of 0.9994 in all cases.

groups are taken from the set of transferable scaling factors of the SQM method.[44] The optimized scaling parameters and the performance of the new scaling scheme are shown in Table 1, where it is compared with the SQM fit, and a modified SQM fit. The latter is one representative example of our extensive fitting attempts within the SQM scheme, with three optimized linear scaling factors s, t, and c (c replaces $\sqrt{s_i s_j}$ in eq 5 when $i \neq j$). The modified SQM fit and the hybrid Lin/Exp scaling fit show much better statistics than the SQM scaling at the price of using two more parameters. The hybrid scheme achieves the best results for the LO modes, which is the key for the prediction of the LO mode frequency of polyyne.

The $k = 0$ LO mode frequency of polyyne cannot be accurately extrapolated from that of oligoynes Ar-$(C\equiv C)_m$-Ar ($2m = 4-20$) because they are not long enough to give reliable predictions for the polymer limit. Therefore, we applied the Lin/Exp scaling scheme with the optimized scaling parameters to the computationally affordable series of H-$(C\equiv C)_m$-H oligoynes ($10 \leq 2m \leq 72$). Figure 6 shows the Lin/Exp scaling results of the in-phase LO mode frequencies of these oligoynes. For comparison, unscaled and SQM scaled results are also shown in the figure. The two nearly parallel curves from unscaled and SQM scaled results show that the SQM scaling does not alter

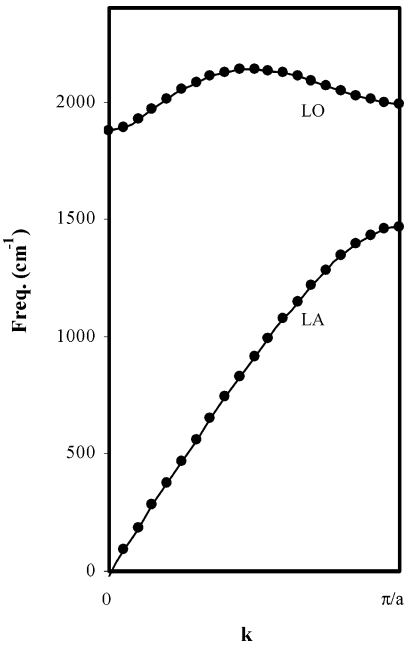

Figure 7. Longitudinal phonon branches of polyyne after the application of the linear/exponential scaling scheme. The unscaled harmonic force constants are obtained from the Hessian of H-$(C\equiv C)_{36}$-H at B3LYP/6-31G* level using the Polycalc approach, including up to 29th unit cell force constant couplings.

the distance-dependent behavior of longitudinal coupling force constants. The crossover between the Lin/Exp scaling curve and those for the unscaled and SQM scaled results is a consequence of the empirically adjusted exponential decay of the longitudinal off-diagonal force constants achieved by the Lin/Exp scheme. A similar scissor shape can be observed between the Lin/Exp scaled and the SQM scaled frequencies in Figure 6, with the former taking the position of the experimental results in the scissor shape present in Figure 4. This signals the improvement in the description of longitudinal coupling off-diagonal force constants and, in turn, it improves the prediction of the in-phase LO mode frequencies by the Lin/Exp scaling scheme. The Raman active LO mode frequency of polyyne is predicted by the Lin/Exp scaling scheme to be 1874 cm^{-1} through the direct oligomer approach.

The Lin/Exp scaled $k = 0$ LO mode frequency was also obtained through the Polycalc approach. The value is determined to be 1877 cm^{-1} by Polycalc based on the Hessian of H-$(C\equiv C)_{36}$-H. Applying an additional extrapolation for the $k = 0$ LO mode frequency in the region of $40 \leq 2m \leq 72$, the frequency is determined to be 1870 cm^{-1} at $1/2m \rightarrow 0$ limit.

In summary, the three different estimates by the Lin/Exp scaling scheme for the $k = 0$ LO mode frequency of polyyne are: (a) 1874 cm^{-1} (direct oligomer frequency extrapolation to infinite chain length), (b) 1877 cm^{-1} (Polycalc values from the longest ($2m = 72$) Hessian available), and (c) 1870 cm^{-1} (extrapolated Polycalc values). These differences indicate the presence of some residual uncertainties and can be used to estimate the intrinsic error of the present algorithm.

The scaled longitudinal phonon dispersion for polyyne is given in Figure 7. The dispersion shows a significant "overbending" character (reduction of frequencies of the optical mode near $k = 0$) an effect that has attracted significant attention recently for graphite,[55,56] reflecting significant nonlocal force constant coupling.

3.4. Further Justifications of the Linear/Exponential Scaling Scheme. By relating stretching force constants and bond

TABLE 2: Bond Length of the Centermost Single and Triple Bonds of H-(C≡C)$_{36}$-H, Predicted by Badger's Rule[a]

methodology		r_1 (C−C) (Å)	r_2 (C≡C) (Å)	δr (BLA) (Å)
Badger's rule (eq 7)	unscaled	1.3246	1.2356	0.0890
	SQM	1.3419	1.2504	0.0915
	modified SQM	1.3388	1.2566	0.0823
	Lin/Exp	1.3724	1.2447	0.1277
optimized geometry	B3LYP	1.3291	1.2414	0.0877
	BH&HLYP	1.3476	1.2139	0.1337

[a] Optimized bond lengths from B3LYP/6-31G* and BH&HLYP/6-31G* calculations are shown for comparison.

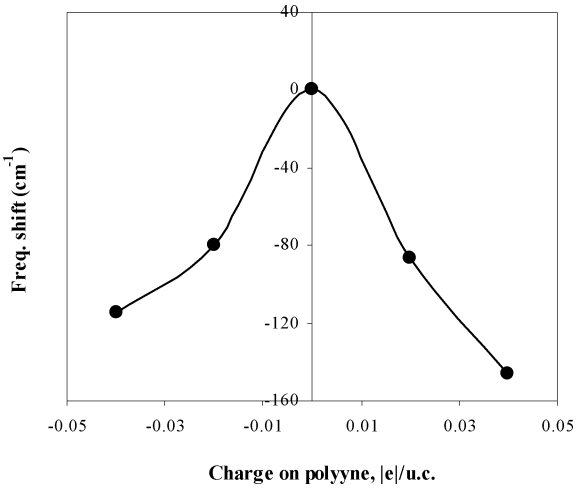

Figure 8. Downshift of the LO mode frequency as a function of additional charge on polyyne, in units of $|e|$ per unit cell (two carbon atoms). Solid-state vibrational calculations were performed at the PBE level using the PWSCF program.

lengths through Badger's rule[57] using Laing and Berry's fitting parameters,[58] we can provide an independent estimate of the C≡C and C−C bond lengths for polyyne. According to Laing and Berry:[58]

$$R_e = (k^{-1/3} + 0.5526)/0.7837 \quad (7)$$

where k is the stretching force constant, in mdyne/Å, of a given carbon−carbon bond, and R_e is the corresponding equilibrium bond length, in Å. The bond lengths estimated from Badger's rule are listed in Table 2. The BLA values are predicted to be 0.08−0.09 Å from the unscaled, SQM scaled, and various modified SQM scaled force constants. On the other hand, the BLA estimated from the hybrid linear/exponential scaled force constants is about 0.13 Å. Note that this alternation value contains both empirical elements and the theoretical force constants of the longest oligoyne. *As such, this is the best currently available BLA value for infinite polyyne.* It is pleasing to note that this alternation value is consistent with the prediction from the BH&HLYP/6-31G* theory, which has been found to be the most reliable method for the prediction of BLA in other highly conjugated carbon systems.[59] It is worth pointing out that the $k = 0$ LO mode frequency of polyyne at the BH&HLYP/6-31G* level is predicted at 2215 cm^{-1} by the direct oligomer approach, extrapolated from the region of $2m = 30-72$ of H-(C≡C)$_m$-H oligoynes. This prediction is too high, which implies that correct BLA is a necessary, but not the only condition for obtaining accurate vibrational frequencies.

A further justification of the hybrid linear/exponential scaling scheme comes from the successful application to the similar conjugated polymer, polyacetylene. PA has two $k = 0$ LO carbon−carbon stretching modes (essentially all in-phase C=C and C−C stretching modes) that couple strongly to BLA. The other six $k = 0$ optical modes are not affected by the longitudinal off-diagonal couplings and can be accurately described by the original[44] SQM scheme. Accurate fitting of both C=C and C−C stretching frequencies of PA *simultaneously* has not been achieved satisfactorily before.[60−62] These two Raman active modes are observed at 1457 and 1066 cm^{-1}, respectively.[61] By applying distance-dependent scaling using the hybrid Lin/Exp scaling scheme to PA, we are able to reproduce these two $k = 0$ LO modes at 1457 and 1067 cm^{-1}, respectively.[63]

4. Concluding Remarks

Finally, we comment on the possible interpretation of the Raman peaks of the encapsulated carbon chains inside multiwalled carbon nanotubes.[10,12] The predicted 1870−1877 cm^{-1} value in this work will be influenced by at least two effects: (a) intrinsic errors of the calculations, and (b) the effect of the tube environment, which might include van der Waals interaction, orbital mixing, and charge transfer (CT). Effect (a) is difficult to estimate. With state-of-the-art theory and use of the longest possible oligomer, the effect is likely to be minimized. The van der Waals effect in (b) is estimated to be around 10 cm^{-1}.[64] The orbital mixing and CT effects vary with tube chirality and are sensitive to the diameter of the tube.[65] CT results in a frequency downshift, which is *qualitatively* illustrated for an isolated polyyne chain in Figure 8, estimated at the PBE level with the PWSCF program.[66] On the basis of this result, we speculate that the lower frequency peak observed at 1825 or 1829 cm^{-1} can be attributed to a slight CT from the nanotube to the carbon chain. The observed upper frequencies at 1850−1860 cm^{-1} agree well with presently calculated $k = 0$ LO mode frequency of polyyne at 1870−1877 cm^{-1} within the uncertainties of the methodology and the presumably small effects of the tube environment assuming little or no CT.

In summary, we obtained a new LO phonon dispersion for polyyne. By introducing a hybrid linear/exponential scaling scheme, the longitudinal Raman active mode of an isolated polyyne chain is determined to be 1870−1877 cm^{-1}. The linear/exponential hybrid scaling scheme performed well for the polyacetylene system[63] as well, and we are planning further applications to polydiacetylene, carotenoids, and other highly conjugated large linear chain molecules and polymeric systems.

Acknowledgment. Support from the U.S. National Science Foundation (grant no. DMR-0331710) and OTKA, Hungary (grant nos. T043685 and K60576) are gratefully acknowledged. We thank Prof. P. Pulay and Dr. G. Csányi for useful comments and Prof. F. Cataldo for sending us the manuscript for his new book on polyyne.

References and Notes

(1) Kertesz, M.; Koller, J.; Azman, A. *J. Chem. Phys.* **1978**, *68*, 2779.
(2) Karpfen, A. *J. Phys. C: Solid State Phys.* **1979**, *12*, 3227.
(3) Kastner, J.; Kuzmany, H.; Kavan, L.; Dousek, F. P.; Kürti, J. *Macromolecules* **1995**, *28*, 344.
(4) Jacquemin D.; Champagne, B. *Int. J. Quantum Chem.* **2000**, *80*, 863.
(5) Poulsen, T. D.; Mikkelsen, K. V.; Fripiat, J. G.; Jacquemin, D.; Champagne, B. *J. Chem. Phys.* **2001**, *114*, 5917.
(6) Peierls R. *Quantum Theory of Solids*; Oxford University Press: Oxford, 1955, p 108.
(7) Kavan, L. *Chem. Rev.* **1997**, *97*, 3061.
(8) *Carbyne and Carbynoid Structures*; Heimann, R. B., Evsyukov, S. E., Kavan L., Eds.; Kluwer: Dordrecht, The Netherlands, 1999.

(9) *Polyynes: Synthesis, Properties, and Applications*; Cataldo F., Ed.; CRC: Boca Raton, FL, 2005.
(10) Zhao, X.; Ando, Y.; Liu, Y.; Jinno, M.; Suzuki, T. *Phys. Rev. Lett.* **2003**, *90*, 187401.
(11) Wang, Z.; Ke, X.; Zhu, Z.; Zhang, F.; Ruan, M.; Yang, J. *Phys. Rev. B* **2000**, *61*, R2472.
(12) Jinno, M.; Ando, Y.; Bandow, S.; Fan, J.; Yudasaka, M.; Iijima, S. *Chem. Phys. Lett.* **2006**, *418*, 109.
(13) Grutter, M.; Wyss, M.; Fulara, J.; Maier, J. P. *J. Phys. Chem. A* **1998**, *102*, 9785; Pino, T.; Ding, H.; Guthe, F.; Maier, J. P. *J. Chem. Phys.* **2001**, *114*, 2208.
(14) Heymann D.; Cataldo, F. Structures and other properties of polyynes and their isomers: theoretical and experimental results. In *Polyynes: synthesis, properties, and applications*; Cataldo, F., Ed.; CRC: Boca Raton, FL, 2005, p 371.
(15) Eisler, S.; Slepkov, A. D.; Elliott, E.; Luu, T.; McDonald, R.; Hegmann, F. A.; Tykwinski, R. R. *J. Am. Chem. Soc.* **2005**, *127*, 2666.
(16) Yang S.; Kertesz, M. *J. Phys. Chem. A* **2006**, *110*, 9771.
(17) Ashcroft, N. W.; Mermin, N. D. *Solid State Physics*; Saunders College: Philadelphia, 1976; Burns, G. *Solid State Physics*; Academic: Boston, 1990.
(18) Higgs, P. W. *Proc. R. Soc. London, Ser. A* **1953**, *220*, 472; Tobin, M. C. *J. Chem. Phys.* **1955**, *23*, 891; Liang, C. Y. *J. Mol. Spectrosc.* **1957**, *1*, 61.
(19) Piseri L.; Zerbi, G. *J. Mol. Spectrosc.* **1968**, *26*, 254.
(20) Cui, C. X.; Kertesz, M. *J. Chem. Phys.* **1990**, *93*, 5257.
(21) Li, S.-Y.; Zhou, H.-H.; Gu, J.-L.; Zhu, J. *Carbon* **2000**, *38*, 929; Ravagnan, L.; Siviero, F.; Lenardi, C.; Piseri, P.; Barborini, E.; Milani, P. *Phys. Rev. Lett.* **2002**, *89*, 285506; Casari, C. S.; Li Bassi, A.; Ravagnan, L.; Siviero, F.; Lenardi, C.; Barborini, E.; Piseri, P.; Milani, P.; Bottani, C. E. *Carbon* **2004**, *42*, 1103; Xue, K.-H.; Tao, F.-F.; Shen, W.; He, C.-J.; Chen, Q.-L.; Wu, L.-J.; Zhu, Y.-M. *Chem. Phys. Lett.* **2004**, *385*, 447.
(22) (a) Liu, Y.; Jones, R. O.; Zhao, X.; Ando, Y. *Phys. Rev. B* **2003**, *68*, 125413. (b) Fantini, C.; Cruz, E.; Jorio, A.; Terrones, M.; Terrones, H.; Van Lier, G.; Charlier, J.-C.; Dresselhaus, M. S.; Saito, R.; Kim, Y. A.; Hayashi, T.; Muramatsu, H.; Endo, M.; Pimenta, M. A. *Phys. Rev. B* **2006**, *73*, 193408.
(23) See, e.g.: Heeger, A. J.; Kivelson, S.; Schrieffer, J. R.; Su, W. P. *Rev. Mod. Phys.* **1988**, *60*, 781.
(24) Kertesz, M.; Choi, C. H.; Yang, S. *Chem. Rev.* **2005**, *105*, 3448.
(25) Löwdin, P.-O. *Adv. Phys.* **1965**, *5*, 1.
(26) Cox, S. B.; Fry, J. L. *J. Comput. Phys.* **1977**, *23*, 42.
(27) Karpfen, A. *Chem. Phys. Lett.* **1979**, *61*, 363.
(28) Suhai, S.; Bagus, P. S.; Ladik, J. *Chem. Phys.* **1982**, *68*, 467.
(29) Kudin, K. N.; Scuseria, G. E. *Phys. Rev. B* **2000**, *61*, 16440.
(30) Frisch, M. J.; Trucks, G. W.; Schlegel, H. B.; Scuseria, G. E.; Robb, M. A.; Cheeseman, J. R.; Montgomery, J. A., Jr.; Vreven, T.; Kudin, K. N.; Burant, J. C.; Millam, J. M.; Iyengar, S. S.; Tomasi, J.; Barone, V.; Mennucci, B.; Cossi, M.; Scalmani, G.; Rega, N.; Petersson, G. A.; Nakatsuji, H.; Hada, M.; Ehara, M.; Toyota, K.; Fukuda, R.; Hasegawa, J.; Ishida, M.; Nakajima, T.; Honda, Y.; Kitao, O.; Nakai, H.; Klene, M.; Li, X.; Knox, J. E.; Hratchian, H. P.; Cross, J. B.; Bakken, V.; Adamo, C.; Jaramillo, J.; Gomperts, R.; Stratmann, R. E.; Yazyev, O.; Austin, A. J.; Cammi, R.; Pomelli, C.; Ochterski, J. W.; Ayala, P. Y.; Morokuma, K.; Voth, G. A.; Salvador, P.; Dannenberg, J. J.; Zakrzewski, V. G.; Dapprich, S.; Daniels, A. D.; Strain, M. C.; Farkas, O.; Malick, D. K.; Rabuck, A. D.; Raghavachari, K.; Foresman, J. B.; Ortiz, J. V.; Cui, Q.; Baboul, A. G.; Clifford, S.; Cioslowski, J.; Stefanov, B. B.; Liu, G.; Liashenko, A.; Piskorz, P.; Komaromi, I.; Martin, R. L.; Fox, D. J.; Keith, T.; Al-Laham, M. A.; Peng, C. Y.; Nanayakkara, A.; Challacombe, M.; Gill, P. M. W.; Johnson, B.; Chen, W.; Wong, M. W.; Gonzalez, C.; Pople, J. A. *Gaussian 03*, revision C.02; Gaussian, Inc.: Wallingford, CT, 2004.
(31) Becke, A. D. *J. Chem. Phys.* **1993**, *98*, 5648.
(32) Choi, C. H. Polycalc, version 0.9.5.06, 1997.
(33) Wilson, E. B., Jr.; Decius, J. C.; Cross P. C. *Molecular Vibrations*; McGraw-Hill: New York, 1955.
(34) Cuff, L.; Cui, C. X.; Kertesz, M. *J. Am. Chem. Soc.* **1993**, *116*, 9269.
(35) Choi C. H.; Kertesz, M. *Macromolecules* **1997**, *30*, 620.
(36) Wong, M. W. *Chem. Phys. Lett.* **1996**, *256*, 391.
(37) Scott, A. P.; Radom, L. *J. Phys. Chem.* **1996**, *100*, 16502.
(38) Hirata, S.; Iwata, S. *J. Chem. Phys.* **1997**, *107*, 10075.
(39) Kudin, K. N.; Scuseria, G. E.; Yakobson, B. I. *Phys. Rev. B* **2001**, *64*, 235406.
(40) Kozlowski, P. M.; Jarzecki, A. A.; Pulay, P.; Li, X. Y.; Zgierski, M. Z. *J. Chem. Phys.* **1996**, *100*, 13985.
(41) Kofranek, M.; Karpfen, A.; Lischka, H. *Int. J. Quantum Chem. Quantum Chem. Symp.* **1990**, *24*, 721.
(42) Irikura, K. K.; Johnson, R. D., III; Kacker, R. N. *J. Phys. Chem. A* **2005**, *109*, 8430.
(43) Pulay, P.; Fogarasi, G.; Pongor, G.; Boggs, J. E.; Vargha, A. *J. Am. Chem. Soc.* **1983**, *105*, 7037.
(44) Baker, J.; Jarzecki, A. A.; Pulay, P. *J. Phys. Chem. A* **1998**, *102*,-1412.
(45) Scemama, A.; Chaquin, P.; Gazeau, M. C.; Benilan, Y. *J. Phys. Chem. A* **2002**, *106*, 3828.
(46) Domingo, C.; Escribano, R.; Murphy, W. F.; Montero, S. *J. Chem. Phys.* **1982**, *77*, 4353.
(47) Guelachvilia, G.; Craig, M.; Ramsay, D. A. *J. Mol. Spectrosc.* **1984**, *105*, 156.
(48) Bjarnov, E.; Christensen, D. H.; Nielsen, O. F.; Augdahl, E.; Kloster-Jensen, E.; Rogstad, A. *Spectrochim. Acta, Part A* **1974**, *30*, 1255.
(49) Dembinski, R.; Bartik, T.; Bartik, B.; Jaeger, M.; Gladysz, J. A. *J. Am. Chem. Soc.* **2000**, *122*, 810.
(50) Hlavaty, J.; Kavan, L.; Kubis, J. *Carbon* **2002**, *40*, 345.
(51) Gibtner, T.; Hampel, F.; Gisselbrecht, J.-P.; Hirsch, A. *Chem.—Eur. J.* **2002**, *8*, 408.
(52) Binsch, G.; Heilbronner, E.; Murrel, J. N. *Mol. Phys.* **1966**, *11*, 305.
(53) Coulson, C. A.; Longuet-Higgins, H. C. *Proc. R. Soc. London, Ser. A* **1947**, *191*, 39; Coulson, C. A.; Longuet-Higgins, H. C. *Proc. R. Soc. London, Ser. A* **1947**, *192*, 16; Coulson, C. A.; Longuet-Higgins, H. C. *Proc. R. Soc. London, Ser. A* **1948**, *193*, 447; Coulson, C. A.; Longuet-Higgins, H. C. *Proc. R. Soc. London, Ser. A* **1948**, *195*, 188.
(54) Longuet-Higgins, H. C.; Salem, L. *Proc. R. Soc. London, Ser. A* **1959**, *251*, 172.
(55) Maultzsch, J.; Reich, S.; Thomsen, C.; Requardt, H.; Ordejon, P. *Phys. Rev. Lett.* **2004**, *92*, 075501.
(56) Piscanec, S.; Lazzeri, M.; Mauri, F.; Ferrari, A. C.; Robertson, J. *Phys. Rev. Lett.* **2004**, *93*, 185503.
(57) Badger, R. M. *J. Chem. Phys.* **1934**, *2*, 128; Badger, R. M. *J. Chem. Phys.* **1935**, *3*, 710.
(58) Laing, J. W.; Berry, R. S. *J. Am. Chem. Soc.* **1976**, *98*, 660.
(59) Wannere, C. S.; Sattelmeyer, K. W.; Schaefer, H. F.; Schleyer, P. v. R. *Angew. Chem., Int. Ed.* **2004**, *43*, 4200.
(60) Kofranek, M.; Lischka, H.; Karpfen, A. *J. Chem. Phys.* **1992**, *96*, 982.
(61) Hirata, S.; Torii, H.; Tasumi, M. *J. Chem. Phys.* **1995**, *103*, 8964.
(62) Hirata, S.; Iwata, S. *J. Chem. Phys.* **1997**, *107*, 10075. Using the oligomer approach up to $C_{50}H_{52}$, and B3LYP/6-31.G* with Gaussian03, we reproduced their frequency values for all optical modes except the in-phase C−C and C═C LO stretching modes. The values are 1017 and 1419 cm^{-1}, respectively, after applying the suggested uniform frequency scaling factor of 0.964.
(63) Yang, S.; Kertesz M. *Chem. Phys. Lett.* **2006**, *432*, 356.
(64) Rao, A. M.; Chen, J.; Richter, E.; Schlecht, U.; Eklund, P. C.; Haddon, R. C.; Venkateswaran, U. D.; Kwon, Y.-K.; Tománek, D. *Phys. Rev. Lett.* **2001**, *86*, 3895.
(65) Rusznyák, Á.; Zólyomi, V.; Kürti, J.; Yang, S.; Kertesz, M. *Phys. Rev. B* **2005**, *72*, 155420.
(66) Baroni, S.; Dal Corso, A.; de Gironcoli, S.; Giannozzi, P.; Cavazzoni, C.; Ballabio, G.; Scandolo, S.; Chiarotti, G.; Focher, P.; Pasquarello, A.; Laasonen, K.; Trave, A.; Car, R.; Marzari, N.; Kokalj, A. http://www.pwscf.org/. The Perdew−Burke−Ernzerhof (PBE) functional was used with 327 eV cutoff energy for carbon and 73 irreducible *k* points.